U. of Iowa 66-11

Negative Ion Detection in the Ionosphere From Effects on ELF Waves*

by

Stanley D. Shawhan**

Department of Physics and Astronomy
University of Iowa
Iowa City, Iowa

March 1966

*Research supported in part by Office of Naval Research Contracts N9onr-93803 and Nonr 1509(06).

**NASA Graduate Trainee.

ABSTRACT

30587

The theory for propagation of small amplitude electromagnetic waves in a cold, homogeneous plasma including negative ions and immersed in a uniform, static magnetic field is developed. It is found that for longitudinal propagation each negative ion introduces a resonance at the negative in gyrofrequency, a concentration dependent cutoff frequency above the negative ion gyrofrequency, and possibly a crossover frequency depending on the ion concentrations and charge to mass ratios. At both the gyrofrequency and the cutoff frequency the group refractive index becomes infinite. Between these two frequencies there is a 'nose' frequency for which the group refractive index is a minimum. Examples are given for a three and five component plasma.

Application of this negative ion theory is made to propagation of negative ion whistlers in the ionosphere. It is found that for frequencies near the negative ion gyrofrequencies the WKB approximation is valid above 300 KM during the nighttime and 150 KM during the daytime. Effects of collisions can be neglected above 150 KM. An ideal experiment is proposed for observation of negative ion whistlers (1-1000 cps). Sample

whistler, frequency-time spectrograms like those which would be observed with such an experiment are sketched. From the distinctive frequencies on these sample spectrograms, it is shown that the negative ion specie and concentration can be determined using the developed cold plasma expressions.

INTRODUCTION

Recently it has been demonstrated that the effects of positive ions on VLF electromagnetic waves propagating in the ionosphere can be used to determine positive ion species, positive ion concentration, and positive ion temperature: Stix [1962] gives expressions for determining the propagation characteristic of a plasma with any number of positive and negative ions; Smith and Brice [1964] developed the theoretical aspects of propagation in a plasma with more than one positive ion; Gurnett, Shawhan, Brice, and Smith [1965] also developed the theory of multicomponent plasmas with particular application to the explanation of the experimentally observed proton whistlers (ion cyclotron whistlers associated with the existence of protons in the ionosphere). Experimental observations of proton whistlers are reported by Shawhan [1966]. Subsequent scaling of proton whistlers observed with the Injun 3 and Alouette 1 satellites has produced measurements of the fractional proton concentration [Shawhan and Gurnett, 1966]; the proton number density, the electron density, and the proton gyrofrequency [Gurnett and Shawhan, 1966]; and the proton temperature [Gurnett and Brice, 1966].

This present work is intended to determine what effects might be observable with a rocket or satellite ELF receiver in the ionosphere due to negative ions and if these negative ion whistlers can be used to identify negative ion species, their concentrations, and temperatures. Consideration has been given previously to the effects of negative ions on whistler mode propagation by Smith [1965], but he considered the limited case of a cold plasma in which the positive and negative ions had the same charge to mass ratio. Teichmann [1965] treated the two component laboratory plasma problems of a heavy positive and heavy negative ion. In a very recent paper Teichmann [1966] has developed the theory for propagation in a cold collisionless plasma with positive and negative ions of different charge to mass ratio. CMA diagrams are calculated for several examples.

This paper is divided into two major parts. Part 1 develops the theory of negative ion effects on the propagation of electromagnetic waves in a cold, homogeneous plasma with a static uniform magnetic field. This theory is treated in detail for the phase and group refractive indices of a three component plasma (e^-, He^-, H^+) for frequencies below the electron gyrofrequency. Extension of the theory is made to multi-component plasmas with a five component

plasma given as an example. In Part 2, application of this theory is made to the inhomogeneous, anisotropic ionospheric plasma and the resultant negative ion whistlers. Consideration is given to the validity of the WKB approximation, the existence of negative ions, and the effects of collisions. Finally sample frequency-time spectrograms are sketched to illustrate negative ion whistler traces and the information about negative ions which can be obtained from them.

PART 1: Theory of Cold Plasma Propagation Including Negative Ions

A. Cold Plasma Expressions; Phase Refractive Index

For the model plasma from which we determine the propagation characteristics of electromagnetic waves including the effects of negative ions we make the following assumptions:

a) temperature is zero for all components

b) plasma is homogeneous in space

c) plasma is immersed in a uniform static magnetic field

d) collisions can be neglected

e) electromagnetic waves are of small amplitude.

With these assumptions the general cold plasma expressions developed by Stix [1962] are applicable. This reference should be consulted for the detailed derivation of these expressions and for their interpretation beyond that given here.

For any number of components in the plasma the following expressions are used to describe the propagation of small amplitude electromagnetic perturbations:

$$R = 1 - \sum_k \frac{\Pi_k^2}{\omega^2} \left(\frac{\omega}{\omega + \Omega_k} \right) \tag{1}$$

$$L = 1 - \sum_k \frac{\Pi_k^2}{\omega^2} \left(\frac{\omega}{\omega - \Omega_k} \right) \tag{2}$$

$$P = 1 - \sum_k \frac{\Pi_k^2}{\omega^2} \tag{3}$$

$$S = \frac{1}{2}(R + L) \tag{4}$$

$$D = \frac{1}{2}(R - L) \tag{5}$$

where

$$\Pi_k^2 = \frac{4\pi n_k Z_k e^2}{m_k} \tag{6}$$

$$\Omega_k = \frac{e_k Z_k B}{m_k c} \tag{7}$$

c speed of light

$e_k Z_k$ charge of k^{th} component including sign

m_k mass of k^{th} component

n_k number density of k^{th} component

Stix has shown that the dispersion relations for propagation along the magnetic field ($\theta = 0$) are given by

$n^2 = R$ right circularly polarized wave

$n^2 = L$ left circularly polarized wave

$P = 0$ longitudinal plasma oscillations

and, for propagation transverse to the magnetic field ($\theta = 90°$) by

$$n^2 = RL/S \qquad \text{ordinary wave}$$

$$n^2 = P \qquad \text{extraordinary wave,}$$

where n^2 is the square of the phase refractive index. For a plasma with electrons, P is large negative and therefore the extraordinary mode is not considered further.

From these dispersion relations the principal resonances, cutoffs, and crossovers can be defined. The frequencies for which $n^2 \to \infty$ are called the principal resonances. At $\theta = 0$ these resonances occur for $R \to \infty$ and $L \to \infty$, the ion gyrofrequencies, and are therefore called the electron and negative ion cyclotron resonances and the positive ion cyclotron resonances, respectively. At $\theta = 90°$ these principal resonances occur at frequencies for which $S = 0$ and are termed the hybrid resonances. Principal cutoffs occur whenever $n^2 \to 0$. For longitudinal and transverse propagation these cutoffs occur at $R = 0$ and $L = 0$. In a homogeneous plasma with a static magnetic field the crossover frequencies [Smith and Brice, 1964] for which $D = 0$ ($n^2 = R = L$) are the frequencies for which both the right and left circularly

polarized waves ($\theta = 0$) become linearly polarized. These cross-over frequencies can exist only in a plasma with more than one ion. In the ionosphere with density and magnetic field gradients, an upward propagating wave changes polarization as the wave passes through the region where the wave frequency is equal to the cross-over frequency. This polarization change from right to left circularly polarized is the key to the explanation of the proton whistler [Gurnett et al., 1965].

Further insight into the meaning of these principal resonances, cutoffs, and crossovers is obtained with the use of a specific model. We now specialize the equations (1) to (5) to the case of a three component plasma. For ease of computation the following dimensionless parameters are defined:

$$\Lambda = \omega/\Omega_+$$

$$\beta = n_-/n_e$$

$$g_+ = m_+e_1/m_1e_+$$

$$g_- = m_-e_1/m_1e_-$$

where Ω_+ is the positive ion gyrofrequency, n_- and n_e are the number density of negative ions and electrons, respectively, and m_+/e_+, m_-/e_-, and m_1/e_1 are the mass to charge ratios of the positive ion, the negative ion and protons, respectively. Because of local charge neutrality ($n_+ = n_e + n_-$), the relative concentration of positive ions to electrons is $1 + \beta$.

Using these dimensionless parameters, equations (1) to (5) become

$$R = 1 + \frac{\Pi_e^2}{\Omega_+\Omega_e} \frac{1}{\Lambda} \left[\frac{1}{(g_+ - \Lambda/1836)} + \frac{\beta}{(g_+ - g_-\Lambda)} - \frac{1+\beta}{g_+(1+\Lambda)} \right] \tag{8}$$

$$L = 1 - \frac{\Pi_e^2}{\Omega_+\Omega_e} \frac{1}{\Lambda} \left[\frac{1}{(g_+ + \Lambda/1836)} + \frac{\beta}{(g_+ + g_-\Lambda)} - \frac{1+\beta}{g_+(1-\Lambda)} \right] \tag{9}$$

$$S = 1 + \frac{\Pi_e^2}{\Omega_+\Omega_e} \left[\frac{1/1836}{(g_+^2 - \Lambda^2/1836^2)} + \frac{g_-\beta}{(g_+^2 - g_-^2\Lambda^2)} + \frac{1+\beta}{g_+(1-\Lambda^2)} \right] \tag{10}$$

$$D = \frac{\Pi_e^2}{\Omega_+\Omega_e} \frac{1}{\Lambda} \left[\frac{g_+}{(g_+^2 - \Lambda^2/1836^2)} + \frac{g_+\beta}{(g_+^2 - g_-^2\Lambda^2)} - \frac{1+\beta}{g_+(1-\Lambda^2)} \right] \tag{11}$$

$$P \simeq 1 - \frac{\Pi_e^2}{\Lambda^2\Omega_+^2} \quad . \tag{12}$$

Neglecting the 1's on the right-hand sides of (8) and (9) and assuming that the positive ion is hydrogen ($g_+ = 1$), we can solve the above equations for the critical frequencies for any given negative ion:

$R = \infty$: $\Lambda = 1836$ electron gyrofrequency

$\Lambda = 1/g_-$ negative ion gyrofrequency (13)

$R = 0$: $\Lambda = (1+\beta+g_-\beta)/g_-$ R wave cutoff (14)

$L = \infty$: $\Lambda = 1$ hydrogen ion gyrofrequency (15)

$L = 0$: doesn't exist for one positive ion

$S = 0$: $\Lambda^2 = (1+g_-\beta+\beta)/(g_-^2\beta+g_-\beta+g_-^2)$

ion-ion hybrid resonance frequency

(dropping the 1 in equation (10)) (16)

$$\Lambda^2 = \frac{\Omega_1\Omega_e}{\left(1 + \Omega_e^2/\Pi_e^2\right)} (1+\beta+\beta/g_-)$$

lower hybrid resonance frequency

(keeping the 1 in equation (10))

$D = 0$: $\Lambda^2 = (1+\beta-g_-^2\beta)/g_-^2$ crossover frequency (17)

For graphing purposes we assume that $\Pi_e = \Omega_e$ which is a good approximation for the ionosphere, and that the negative ion has $g_- = 4$ (which is He^- although it is not observed to exist in its ground state). Figure 1 and Figure 2 show plots of $n^2 = R$, $n^2 = L$, and $n^2 = RL/S$ for two different values of β, the negative ion fractional concentration. Also shown are the appropriate phase velocity surfaces for the frequency range between each of the critical frequencies. A phase velocity surface is the plot of phase velocity vs angle from the magnetic field direction (which is vertical in Figures 1 and 2). The plus or minus signs indicate the branch of n^2 which is right circularly polarized (R) and which is left (L) at $\theta = 0$. Stix [1962] should be consulted for the detailed transition properties of these surfaces between frequency intervals.

It can be shown at zero frequency, $\Lambda = 0$, that $R = L = n_A^2$ where n_A is the Alfvén phase refractive index for longitudinal propagation. With increasing frequency in Figure 1 the R wave reaches a resonance at $\Lambda = 0.25$ which is the He^- gyrofrequency. For frequencies between the He^- gyrofrequency and $R = 0$ at $\Lambda = 0.375$, the R wave cannot propagate. Above $R = 0$ the L wave reaches a

resonance at $\Lambda = 1$ which is the hydrogen ion gyrofrequency and above the H^+ gyrofrequency the L wave cannot propagate until just below the electron gyrofrequency. The R wave, however, can propagate for all frequencies above R = 0 up to the electron gyrofrequency where a principal resonance occurs. In Figure 2 $\beta = 0.05$. The principal resonances occur again at the gyrofrequencies; the R = 0 cutoff frequency is slightly lower than in Figure 1 because β is less. For this choice of β, however, a crossover frequency appears at $\Lambda = 0.125$; at this frequency R = L. The phase velocity surfaces indicate that in going across D = 0 the labels for the R and L waves are exchanged. With increasing frequency the fast R wave becomes the slower wave.

The case of a negative ion and a positive ion can be contrasted with the case of two positive ions as discussed by Smith and Brice [1964] and Gurnett et al. [1965]. In the case of two positive ions the R wave can propagate for all frequencies up to the electron gyrofrequency; there are no other resonances and no 'stop bands' where the R wave cannot propagate (as between $R = \infty$ and R = 0 in Figures 1 and 2). Also, the crossover frequency (for which D = 0) always exists for two or more positive ions and occurs between the positive ion gyrofrequencies. From

Figures 1 and 2, however, we find that the existence of a crossover frequency depends on the concentration of the negative ion and that if D = 0 exists, it occurs below the negative ion gyrofrequency for $g_- > g_+$. For the case that $g_+ > g_-$ (positive ion is heavier) the crossover frequency for which D = 0 occurs when both waves are evanescent; at a frequency between R = ∞ and R = 0 where $n_L^2 = L < 0$, $n_R^2 = R < 0$.

For the case of $\theta = 90°$, transverse propagation, the extraordinary wave can propagate for frequencies from zero frequency (where $n_X^2 = X = n_A^2$) up to the ion-ion hybrid resonance which occurs between R = ∞ and R = 0. A narrow stop band of frequencies occurs between S = 0 and R = 0. Above R = 0 propagation is allowed up to the lower hybrid resonance (near 30 Λ in Figures 1 and 2). As can be seen from Figures 1 and 2 and from equation (16), the exact frequency of these hybrid resonances depends on the negative ion concentration, but these hybrid resonances always occur between adjacent gyrofrequencies. For the case of two positive ions these transverse resonances depend similarly on concentration of the positive ions but the ion-ion hybrid resonance occurs between the L = ∞ and L = 0 frequencies.

By use of equations (1) to (5), relations for the phase refractive index can be obtained for any number of positive and negative ions. To discover what effect additional negative and positive ions have on the phase refractive indices a five component plasma is considered. Figure 3 illustrates the phase refractive indices for a plasma containing electrons and O_2^-, O^-, He^+, O^+ ions with the fractional concentrations as given in the figure. Because of the two positive ions, resonances occur at the positive ion gyrofrequencies and a L = 0 cutoff occurs between the two gyrofrequencies. Because of the two negative ions and electrons three resonances occur, two at the negative ion gyrofrequencies and the other at the electron gyrofrequency. The three negative components produce two R = 0 cutoffs, each between the adjacent negative component gyrofrequencies. With this choice of plasma components only one D = 0 frequency occurs. This D = 0 occurs between the O^- and He^+ gyrofrequency and at a frequency for which both waves are evanescent. For transverse propagation the lower hybrid resonance and two ion-ion hybrid resonances occur. These ion-ion hybrid resonances occur between the O_2^- gyrofrequency and the R = 0 frequency just above it, and between the O^+ gyrofrequency and the L = 0 frequency just above

it. The lower hybrid frequency is again at approximately 30 Λ. As in the three component case, the exact hybrid resonant frequencies are determined by the concentrations of all the components as are the cutoff frequencies.

In conclusion, it has been found that for longitudinal propagation the inclusion of negative ions in a plasma introduces a resonance at the ion gyrofrequency and a cutoff above this gyrofrequency at a frequency determined by the concentrations of all the plasma components. Frequency stop bands exist for each wave between a gyrofrequency and the next higher cutoff frequency for that wave. In addition a frequency for which $n^2 = R = L$ (the right and left circularly polarized waves become linearly polarized and indistinguishable) may occur. This D = 0 crossover frequency occurs only when both waves are evanescent (non-propagating) for the negative ion gyrofrequency being higher than the positive ion gyrofrequency of an adjacent negative ion-positive ion pair ($\Omega_- > \Omega_+$). For the case of $\Omega_- < \Omega_+$ the D = 0 crossover frequency may occur below Ω_- for small negative ion concentrations. Resonances for transverse propagation are concentration dependent and occur between each ion gyrofrequency and the next higher cutoff frequency. A stop band for transverse propagation exists between the resonance frequency and this next higher cutoff frequency.

B. Group Refractive Index

Plots of the phase refractive indices for the right and left circularly polarized longitudinally propagating waves have provided identification of the principal resonance, cutoff, and crossover frequencies. Experimentally the quantity measured for electromagnetic waves propagating in a plasma is the group delay time as a function of frequency, $t(\omega)$. The group delay time is defined by the integral

$$t(\omega) = \frac{1}{c} \int_{path} n_g(\omega)\, ds \tag{18}$$

where $n_g(\omega)$ is the group refractive index. For whistlers in the ionosphere over a limited frequency range, equation (18) can be evaluated to give the Eckersely dispersion law, $t(\omega) = Df^{-1/2}$ [Helliwell, 1965], where D is the dispersion constant and f the frequency. In terms of the dimensionless frequency, the group refractive index is given by

$$n_g = n + \Lambda \frac{\partial n}{\partial \Lambda} \quad (\theta = 0) \ . \tag{19}$$

For the ideal cold plasma that has been considered, the group refractive index is, however, independent of the propagation path. Therefore the group time delay for a given frequency can be written as

$$t(\omega) = n_g \frac{S}{c} \tag{20}$$

which is the group refractive index scaled by the ratio of the path length S to the velocity of light in a vacuum.

Figure 4 is a plot of Λ vs n_g for two different negative ion concentrations, $\beta = 0.05, 0.10$. The expressions for the group refractive index of the three component plasma (e^-, He^-, H^+) can be derived from equation (8) and (9) by using equation (19). For the right and left circularly polarized waves the group refractive indices are as follows:

$$n_g(R) = \frac{\Pi_e}{2(\Omega_1\Omega_e\Lambda)^{1/2}} \frac{\left[1 + \frac{\beta}{(1-4\Lambda)^2} - \frac{1+\beta}{(1+\Lambda)^2}\right]}{\left[1 + \frac{\beta}{(1-4\Lambda)} - \frac{1+\beta}{(1+\Lambda)}\right]^{1/2}} \qquad (21)$$

$$n_g(L) = \frac{-\Pi_e}{2(\Omega_1\Omega_e\Lambda)^{1/2}} \frac{\left[1 + \frac{\beta}{(1+4\Lambda)^2} - \frac{1+\beta}{(1-\Lambda)^2}\right]}{\left[1 + \frac{\beta}{(1+4\Lambda)} - \frac{1+\beta}{(1-\Lambda)}\right]^{1/2}} \qquad (22)$$

for frequencies near the ion gyrofrequencies. From observation of the plots of equations (21) and (22) in Figure 4 it is seen that $n_g(L)$ becomes infinite at the proton gyrofrequency. From equation (2), then, the group delay time becomes infinite and the

wave frequency equal to the hydrogen ion gyrofrequency never reaches the detector. Likewise the group refractive index (time delay) becomes infinite for the R wave at the He^- gyrofrequency. The feature of the group refractive index different from the phase refractive index is the effect of the cutoff frequency. Because the group refractive index, given by equation (19), involves the derivative of n with respect to Λ, the group refractive index becomes infinite at a cutoff frequency (R = 0, or L = 0) also. Therefore, as shown in Figure 4, the group refractive index (time delay) for the right circularly polarized wave becomes infinite as the frequency decreases down to the R = 0 cutoff frequency. With increasing negative ion concentration the stop band of frequencies between the negative ion gyrofrequency and the cutoff frequency above it becomes larger. The frequency of the cutoff is given by equation (14). One more feature of the group refractive index is illustrated by Figure 4. For frequencies below the negative ion gyrofrequency a minimum in n_g can occur for one of the waves. This minimum in the group refractive index implies a minimum in the time delay. We call this frequency for which n_g is a minimum the 'nose' frequency in analogy with the nose frequency observed with electron

whistlers at high latitudes [Helliwell, et al., 1956]. For $\beta = 0.05$ the nose occurs in the R wave at the frequency marked in Figure 4. For $\beta = 0.10$ the nose appears in the L wave. From Figures 1 and 2 and equation (17) it can be shown that if a crossover frequency for D = 0 exists, then the nose occurs in the R wave; if no D = 0 crossover frequency exists, then the nose occurs in the L wave. Note that the frequency for which the R and L wave traces cross for the group refractive index is not the D = 0 crossover frequency.

From the discussion of Figure 3 it was learned that the inclusion of addition negative ions introduced additional resonances at the respective negative ion gyrofrequencies and additional R = 0 cutoffs at frequencies determined by the ion concentrations. Based on the knowledge gained from the discussion of Figure 4 and from the positions of the resonances and cutoff in Figure 3, Figure 5 is a sketch of the group refractive index for the five component plasma. With three negative components (e^-, O_2^-, O^-) two stop bands for the R wave exist just above the negative ion gyrofrequencies. No R wave can propagate in these stop bands. Likewise the two positive ions cause an L wave stop band just above the O^+ gyrofrequency. Above the He^+ gyrofrequency

no L wave can propagate for any frequency up to a L = 0 cutoff near the electron gyrofrequency. Note that a nose frequency must always exist for R or L waves between a cutoff and a resonance frequency.

It has been found, in conclusion, that the group refractive index, related to the experimentally observed group delay time by equation (18), becomes infinite at the principal resonances and cutoffs for longitudinally propagating R and L waves. Since the cutoff frequencies are concentration dependent, observation of these cutoff frequencies for all the waves (negative and positive ion whistlers) can be used with expressions like equation (14) to determine the concentrations of all the ions in the plasma.

PART 2: Application of Theory to Negative Ion Whistlers in the Ionosphere for the Determination of Negative Ion Species and Concentrations

The theoretical treatment of the effects of negative ions on the phase and group refractive indices and the resulting propagation characteristics of electromagnetic waves is now considered in application to negative ion whistlers propagating in the ionosphere. In particular we want to establish to what extent the negative ion whistler propagation characteristics due to the effects of negative ions discussed in Part 1 can be of use in ionospheric research. Specifically, this section illustrates the effects observable with a rocket or satellite ELF receiver in the ionosphere due to negative ions and that these negative ion whistlers can be used to identify negative ion species and their respective concentrations.

A. Existence of Negative Ions in the Ionosphere

A recent paper by Whitten et al. [1965] reports the presence of an unidentified negative ion in the D-region (50-80 KM) which is assumed to be O_2^- by may be O^-. Very recently de Mendonca has flown a Nike-Apache rocket on which was an experiment to determine

positive and negative ion concentrations [R. A. Helliwell, private communication, 1966]. Results of this experiment are not yet available. In a review article [Branscomb, 1964], Branscomb states that 'the role of negative ions in atmospheric physics is most dramatically demonstrated by the polar cap absorption event'. In general, however, very few experimental observations of negative ions in the ionosphere have been made. Taking these references as evidence that negative ions exist in the ionosphere, it is left, therefore, to determine the effects of these negative ions on ELF waves to produce negative ion whistlers and the information to be gained from these negative ion whistlers.

Branscomb [1964] considers that O_2^-, O^-, H^-, C^-, NO_2^-, O_3^-, OH^-, HO_2^-, and N_3^- may be negative ions of importance in the ionosphere. Because of their respective scale heights and neutral abundances, above 50 KM probably only O_3^-, O_2^-, OH^-, O^-, and H^- could exist in any significant concentration. Table 1 gives the measured $\beta(O_2^-)$ values of Whitten et al. [1965] and a suggestion of other negative ions that might exist at the given altitudes.

B. Validity of WKB Approximation

In order to quantitatively apply the propagation theory developed in Part 1 to the case of the ionospheric plasma, one must test the validity of the WKB approximation. The condition that the WKB approximation be valid is given by

$$r = \frac{1}{n^2} \frac{dn}{dh} \frac{c}{\omega} \ll 1 \qquad (23)$$

where n is the phase refractive index, h the altitude, ω the wave frequency (sec^{-1}) and c the speed of light in a vacuum. If the condition (23) is satisfied then the same plane wave solution that was assumed for the development in Part 1 is also valid for treatment of propagation in the ionosphere. Also, the local plasma parameters can be used in the cold plasma equations of Part 1. If r is large compared to 1, then a full wave solution must be used for quantitative results. As can be seen from equation (23), a small refractive index, a low frequency, a large change of the refractive index with altitude, or a combination of these factors could cause $r \gtrsim 1$.

Calculations of r in equation (23) have been made for a nighttime electron density profile shown in Figure 7. This nighttime profile provides the largest possible changes of n with

altitude below 300 KM since the daytime profile tends to be filled in smoothly between 100 and 300 KM. Assuming a wave frequency of 20 cps and the presence of the O_2^- ion, r is equal to 0.35 at 150 KM and 0.18 at 250 KM. For a frequency of 45 cps and O^- at 350 KM r = 0.009 (see Table 1). In all three cases $r < 1$. For the proton whistler at 600 KM r = 0.009 and the WKB approximation appears to be valid for this case since the quantitative results of concentration and temperatures from proton whistlers agree well with other experimental methods (see references given in Introduction). It appears therefore that down to approximately 300 KM at night the WKB approximation is valid without question; below 300 KM it may be that quantitative measurements with negative ion whistlers may not be strictly valid. As the electron density profile begins to fill in during the daytime, quantitive measurements should be good to approximately 150 KM.

C. Effects of Collisions

In the ionosphere the effect of neutral-ion and ion-ion collisions can cause collisional damping of the propagating negative ion whistlers and can affect the quantitative results derived in Part 1. Stix [1962] has shown that the effects of

collisions can be included in the equations (1) to (5) through the phenomenological collision frequency ν by substitution of $m_k (1 + i\omega/\nu_k)$ for m_k where m_k is the mass of the k^{th} specie, and ν_k is the collision frequency for the k^{th} specie. According to Nicolet [1953] and Sachs [1965] the ion and electron collision frequencies are approximately related by $\nu_k^2 = (m_e/m_k)\nu_e^2$ where m_e and ν_e are the electron mass and collision frequency, respectively. Using the substitution suggested by Stix and the collision frequency relation in equation (1) specialized to three components, we obtain for the real part of the R wave phase refractive index

$$\mathrm{ReR} = \frac{1836}{\Lambda}\left[\frac{1}{(Z^2/1836^2 + 1)} + \frac{\beta\,(1 - g_-\Lambda)}{(g_-^2\Lambda^2 + (g_-/1836)Z^2 - 2g_-\Lambda + 1)}\right.$$

$$\left. - \frac{(1+\Lambda)\,(1+\beta)}{(\Lambda^2 + Z^2/1836 + 2\Lambda + 1)}\right] \qquad (24)$$

where $\Lambda = \omega/\Omega_1$, $g_+ = 1$, and $Z = \nu_e/\Omega_1$.

Figure 6 is a plot of equation (24) for $g_- = 4$ and for $Z^2 = 1$, and 10. It can be seen for $Z^2 = 10$ that the resonant frequency is shifted to a lower frequency and that no cutoff frequency exists. For $Z^2 = 1$, however, the resonant frequency

is only slightly shifted and a cutoff frequency still exists. We conclude from Figure 6, therefore, that for values of $Z^2 < 1$, the results obtained in Part 1 neglecting collisions are essentially correct. In Table 1 are given values of Ω_1 for mid latitudes and of measured and calculated values of ν_e from Helliwell [1965]. Values of Z^2 are listed for each altitude. At 150 KM and above, $Z^2 < 1$ so that the effects of collisions can be neglected above 150 KM. The resonances and cutoffs occur as described in Part 1.

D. Sample Spectrograms with Negative Ion Effects

It has been shown that above approximately 150 KM during the daytime and 300 KM during the nighttime the propagation characteristic developed for an ideal cold, homogeneous plasma with a uniform, static magnetic field can be applied to the ionospheric plasma. Figures 4 and 5 were suggestive of frequency-time whistler spectrograms that would be observed in the ideal plasma. In the ionosphere the magnetic field and ion concentrations change with altitude and latitude so that, for a given wave frequency ω, Λ changes with altitude and latitude as does the plasma frequency. To determine the type of frequency-time whistler spectrogram that we might expect to observe experimentally we use the model

ionosphere shown in the top of Figure 7. The electron density profile is typical for nighttime. A He^- negative ion is assumed, to be consistent with Figures 1 and 2, but the He^- ion cannot exist in the ionosphere in its ground state. For illustration, the positive ion is taken as H^+ with a concentration given by $n(H^+) = n_e(1+\beta)$. The $\beta(He^-)$ profile is designed to have a maximum of 0.1. Equations (13), (14), (15), and (17) are used to compute the critical frequencies $L = \infty$, $R = 0$, $R = \infty$, and $D = 0$ as the magnetic field and β change with altitude. A plot of these frequencies is shown in the bottom of Figure 7.

In Figure 7 the regions with positive sloping lines are regions where right circularly polarized (R) waves can propagate. The negative sloping lines indicate regions of left circular polarized (L) wave propagation ($\theta = 0$). From the principal frequency diagram of Figure 7 and the feeling for the group refractive index from Figure 4 and Figure 5 we can pick an altitude and sketch a frequency-time spectrogram by roughly integrating equation (18). Sketched frequency-time spectrograms of whistlers initiated by a lightning impulse at the base of the ionosphere are shown in Figure 8 for three different altitudes for both an initial R wave and an initial L wave.

For example, we construct the whistler spectrogram at altitude A for an initial R wave. For all frequencies above R = 0 (220 cps) the R wave can propagate. For frequencies decreasing to 220 cps the time delay becomes infinite. Frequencies between R = 0 and the maximum frequency for which D = 0 (200 cps) never reach the satellite or rocket at altitude A because they run into R = 0 and the delay times become infinite as shown in Figure 8. Frequencies between D = 0 MAX (200 cps) and the D = 0 crossover frequency at altitude A, all pass through D = 0 and change from right to left circularly polarized (L) waves. These L wave delay times become shorter than the R wave delay times would be for frequencies close to the R = 0 frequency since the L wave is faster. Below the crossover frequency for D = 0 at altitude A the wave is right circularly polarized. Since the wave polarization changes at D = 0, the observed traces above and below D = 0 are markedly different.

For the last example, the spectrogram at altitude C for an initial left circularly polarized wave is constructed at shown in Figure 8. Above the maximum crossover frequency for which D = 0, the L wave can propagate but is resonant at the hydrogen ion (proton) gyrofrequency. Between the frequency of D = 0 MAX and R = ∞ (He^- gyrofrequency)

at altitude C the wave has changed polarization in passing the altitude for which D = 0 and is absorbed at the He^- gyrofrequency along the path. Between the He^- gyrofrequency and the crossover frequency, polarization of the wave is right circular which has increasing time delay for frequencies approaching R = ∞. Below D = 0 the polarization is changed to left circular. These spectrograms in Figure 8 are representative of the type of whistler spectrograms that could be observed if negative ions exist in the ionosphere above 150 KM.

We now reverse the procedure and study these sample whistler spectrograms to find out what information about negative and positive ions can be obtained with experimentally observed spectrograms such as these. An ideal ELF receiver for this experiment would have a frequency response between a few cps and 1000 cps for three orthogonal magnetic loop antennas and three orthogonal electric dipole antennas. This frequency response covers the ion gyrofrequencies in the negative ion region of the ionosphere and the orthogonal antennas allow polarization measurements to be made. A three axis magnetometer would be needed to determine the geomagnetic field vector. The magnetic receivers are best for observation of the resonances at the gyrofrequencies

since the magnetic fields of the waves become large. But, the electric receivers are better for observation of the cutoffs and hybrid resonances since the electric fields become large. The resulting spectrograms would contain information on ion species, ion concentration, and ion temperature. For example, consider again the spectrogram in Figure 8 for an initial R wave at altitude A. First it can be determined immediately that negative ions are present at altitude A since the electron whistler trace (R) has a nearly infinite delay time at approximately 200 cps. With no negative ions this trace would go to zero frequency and have no infinite time delays. Once it is established that, below the maximum crossover frequency D = 0 MAX, part of the wave is an L wave, the negative ion can be identified since, at the base of the ionosphere, D = 0 MAX (upper frequency where L wave stops) and the negative ion gyrofrequency are coincident. This gyrofrequency identifies the charge to mass ratio of the negative ion. Measurement of the R = 0 cutoff frequency (asymptotic to the electron whistler trace) and the D = 0 frequency (discontinuity in the traces at approximately 100 cps) with knowledge of the negative ion charge to mass ratio can give the positive ion charge to mass ratio and the concentrations of the negative and positive ion with

respect to the electron concentration. For the three component plasma this determination of β and the positive ion charge to mass ratio (g_+) can be made by solving the more generalized forms of equations (14) and (17); two unknowns and two equations exist. Likewise the other sample whistler spectrograms can be treated to extract information about negative and positive ions using the theory developed in Part 1. Extension of the theory can be made to include more negative and positive ions. The spectrograms will contain more resonances, cutoffs, and crossover frequencies to supply the information necessary to idenify the ions and their concentrations. Information about the negative ion temperature might be obtainable from cyclotron damping of the negative ion whistler (R wave) near the resonance in the manner used by Gurnett and Brice [1966] for the proton whistler. At low altitudes, however, collisional damping may dominate in which case it would be possible to determine the ion collision frequency, but not the temperature.

It has been shown that experimentally observed ELF whistler spectrograms represented by those in Figure 8 can be used with the theoretical development in Part 1 [equations (1) to (5) and (13) to (17)] to determine the negative and positive ion species and their concentrations with respect to the electron density at the altitude of observation with a rocket or satellite.

CONCLUSIONS

Part 1: Theory of Cold Plasma Propagation Including Negative Ions

Propagation characteristics for electromagnetic waves have been treated for the case of a cold homogeneous multi-component plasma immersed in a static, uniform magnetic field. Consideration was given to both the phase and the group refractive index when negative ions were included with the following conclusions:

(1) A resonance occurs for the right circularly polarized (R) wave at the gyrofrequency for each of the negative ions and for longitudinal propagating waves ($\theta = 0$).

(2) An R wave ($\theta \approx 0$) cannot propagate for frequencies between the negative ion gyrcfrequency ($R = \infty$) and the cutoff frequency ($R = 0$) above this gyrofrequency. The width of this stop band is dependent on the concentrations of all the components in the plasma and increases as the negative ion concentration increases.

(3) For the case that negative and positive ions exist in the plasma and that at least one negative ion is heavier than a positive ion, a frequency $D(\Lambda) = 0$ may exist.

At this crossover frequency the right and left circularly polarized waves ($\theta = 0$) become linearly polarized. As the negative ion concentration increases the crossover frequency may become non-existent.

(4) For transverse propagation ($\theta = 90°$) hybrid resonances occur between a negative ion gyrofrequency and an R wave cutoff frequency. This resonance frequency depends on the ion concentrations as does the lower hybrid resonance above the highest ion gyrofrequency but below the electron gyrofrequency.

(5) The integral of the group refractive index along the ray path gives the experimentally observed whistler delay time $t(\Lambda)$. This group refractive index becomes infinite at the negative ion gyrofrequency and at the R wave cutoff frequency. Between these two frequencies the wave is evanescent (non-propagating) and is not observable.

Part 2: Application of Theory to Negative Ion Whistlers in the Ionosphere for the Determination of Negative Ion Species and Concentrations

(1) To apply the negative ion whistler theory of Part 1 quantitatively to the ionospheric plasma the WKB approximation must be valid. At nighttime because of large electron density gradients the approximation appears to be good above 300 KM; during the daytime above 150 KM because the gradients become smaller.

(2) Effects of collisions can be neglected above 150 KM during both daytime and nighttime.

(3) If negative ions exist in a significant concentration above 300 KM during the nighttime or above 150 KM during the daytime, effects on right circularly polarized ELF waves would be observable. Above these altitudes quantitative measurements of experimental negative ion whistler frequency-time spectrographs can give information on negative ion specie and concentration when used with the equations developed in Part 1.

REFERENCES

Branscomb, Lewis M., A review of photodetachment and related negative ion processes relevant to aeronomy, Annales de Geophysique, 20 (1), 88-105, 1964.

Gurnett, Donald A., and Neil M. Brice, Cyclotron damping of ion cyclotron whistlers: a method for the determination of ion temperature, J. Geophys. Res., (to be published), 1966.

Gurnett, Donald A., and Stanley D. Shawhan, Determination of hydrogen ion concentration, electron density, and proton gyrofrequency from the dispersion of proton whistlers, J. Geophys. Res., 71 (3), 741-754, 1966.

Gurnett, D. A., S. D. Shawhan, N. M. Brice, and R. L. Smith, Ion cyclotron whistlers, J. Geophys. Res., 70, 1665-1706, 1965.

Helliwell, Robert A., Whistlers and Related Ionospheric Phenomena, Stanford University Press: Stanford, 1965.

Helliwell, R. W., J. H. Crary, J. H. Pope, and R. L. Smith, The 'nose' whistler--a new high latitude phenomenon, J. Geophys. Res., 61 (1), 139-142, 1956.

Nicolet, Marcel, The collision frequency of electrons in the ionosphere, J. Atmos. Terr. Phys., 3, 200-211, 1953.

Sachs, D. L., Effects of collisions on ion cyclotron waves, Physics of Fluids, 8, 1520-1530, 1965.

Shawhan, S. D., Experimental observations of proton whistlers from Injun 3 VLF data, J. Geophys. Res., 71 (1), 29-45, 1966.

Shawhan, Stanley D., and Donald A. Gurnett, Fractional concentration of hydrogen ions in the ionosphere from VLF proton whistler measurement, J. Geophys. Res., 71 (1), 47-59, 1966.

Smith, Jack, Negative ion effects on whistler mode propagation, J. Geophys. Res., 70, 53-59, 1965.

Smith, R. L., and Neil Brice, Propagation in multicomponent plasmas, J. Geophys. Res., 69, 5029-5040, 1964.

Stix, Thomas Howard, The Theory of Plasma Waves, McGraw-Hill Book Co., Inc.; New York, 1962.

Teichmann, J., On the propagation of electromagnetic waves in a plasma with heavy positive and negative ions, Physics Letters, 19 (7), 534-536, 1965.

Teichmann, J., On the propagation of electromagnetic waves in a plasma with negative ions, Research Report, Département de Physique, Université de Montréal, Montréal, Canada, March 1966.

Whitten R. C., I. G. Poppoff, R. S. Edmonds, and W. W. Berning, Effective recombination coefficients in the lower ionosphere, J. Geophys. Res., 70, 1737-1742, 1965.

TABLE 1

LOWER IONOSPHERE DATA

Alt. KM	Positive Ions cm^{-3}	Negative Ions	r WKB Validity	Ω_1 sec^{-1}	ν_e sec^{-1}	Z^2
50		$\beta\ (O_2^-) = 10^2$ $[O_3^-, O^-, OH^-]$		5.5×10^3	1×10^8	3×10^8
100		$\beta\ (O_2^-) = 10^{-3}$ $[O^-, OH^-]$		5.4×10^3	1×10^5	3×10^2
150		$[O^-, OH^-]$	O_2^- at 20 cps 0.35	5.3×10^3	3×10^5	0.3
200				5.3×10^3	4×10^2	5.7×10^{-3}
250	O^+ 8×10^4 He^+ 5×10^3	$[O^-, H^-]$	O_2^- at cps 0.18	5.2×10^3		
300	O^+ 3×10^5 He^+ 7×10^4			5.14×10^3	7×10^2	10^{-3}
350	O^+ 3×10^5 He^+ 9×10^4 O^+ 2×10^5	$[H^-, O^-]$	O^- at 45 cps 0.009	5.1×10^3		
400	He^+ 1×10^4 H^+ 2×10^3			5.0×10^3	6×10^2	10^{-3}

TABLE 1 (CONT'D)

Alt. KM	Positive Ions cm^{-3}	Negative Ions	r WKB Validity	Ω_1 sec^{-1}	ν_e sec^{-1}	Z^2
450	O^+ 1 x 10^5 He^+ 1 x 10^4 H^+ 3 x 10^3	$[H^-]$		4.9 x 10^3		
500	O^+ 6 x 10^4 He^+ 2 x 10^4 H + 5 x 10^3			4.85 x 10^3	5 x 10^2	10^{-2}
550	O^+ 3 x 10^4 He^+ 2 x 10^4 H + 6 x 10^3			4.8 x 10^3		

FIGURE CAPTIONS

Figure 1. Phase refractive index squared vs frequency for a plasma containing e^-, He^-, H^+ with a negative ion fractional concentration of $\beta = 0.10$.

Figure 2. Phase refractive index squared vs frequency for a plasma containing e^-, He^-, H^+ with a negative ion concentration of $\beta = 0.05$.

Figure 3. Phase refractive index squared vs frequency for a plasma containing e^-, O^-, O_2^-, O^+, He^+.

Figure 4. Group refractive index vs frequency for a plasma containing e^-, He^-, H^+ with $\beta = 0.05$, $\beta = 0.10$.

Figure 5. Sketched group refractive index vs frequency for a plasma containing e^-, O^-, O_2^-, O^+, He^+.

Figure 6. Effect of collisions on the phase refractive index squared vs frequency at a resonance and a cutoff for $Z^2 = 1, 10$, $Z = \nu_e/\Omega_1$.

Figure 7. A model ionosphere of e^-, He^-, H^+ and a plot of the critical frequencies against altitude for longitudinal propagation.

Figure 8. Sketches of frequency-time spectrograms for an ionospheric plasma of e^-, He^-, H^+ at three different altitudes and for both an initial right circularly polarized and left circularly polarized wave.

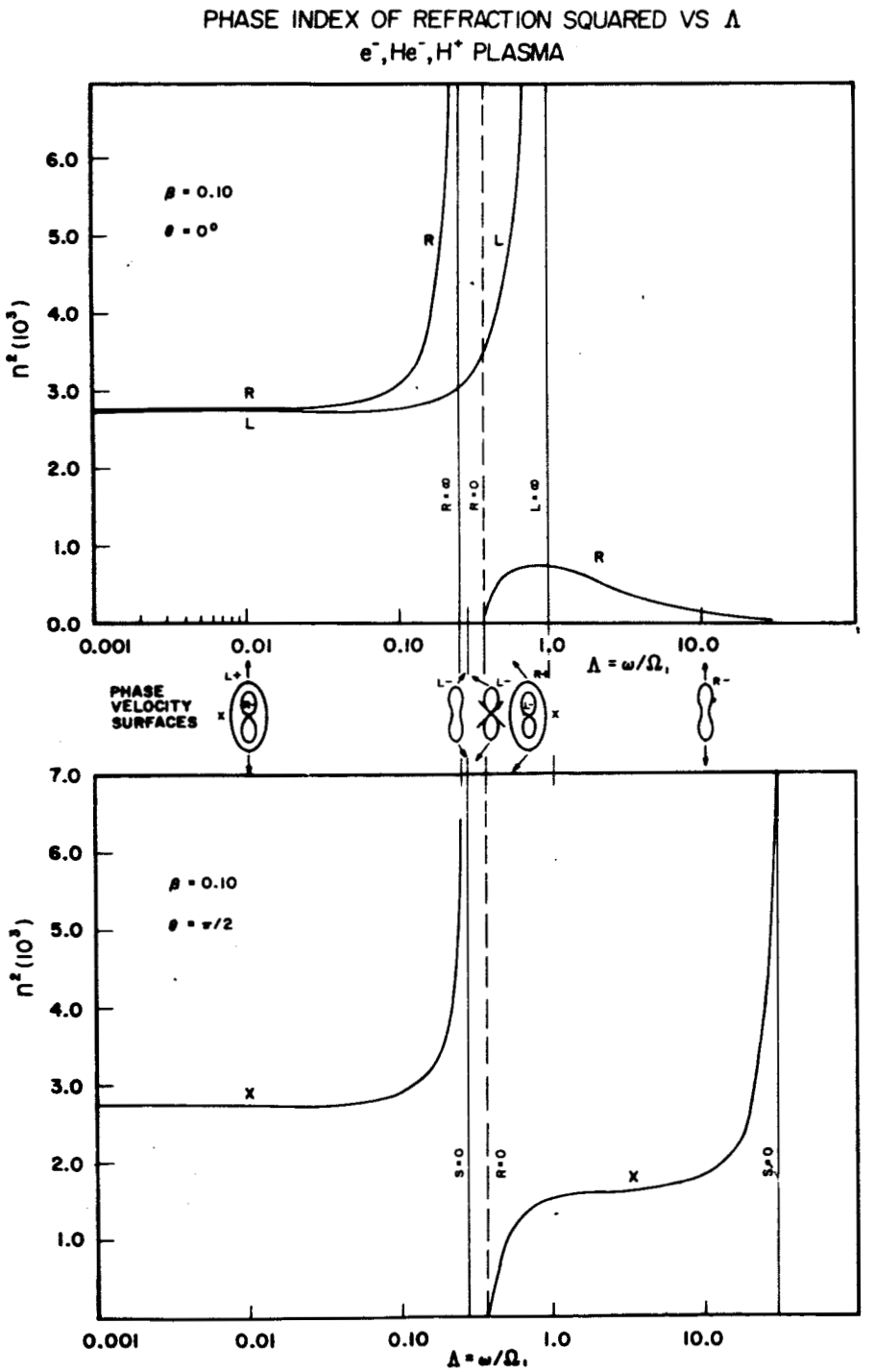
PHASE INDEX OF REFRACTION SQUARED VS Λ
e⁻,He⁻,H⁺ PLASMA
β = 0.10
θ = 0°
R
L
R
L
R=∞
R=0
L=∞
R
n²(10³)
6.0
5.0
4.0
3.0
2.0
1.0
0.0
0.001
0.01
0.10
1.0
10.0
Λ = ω/Ω,
PHASE VELOCITY SURFACES
L+
R+
L-
R-
X
β = 0.10
θ = π/2
X
S=0
R=0
X
S=0
7.0
6.0
5.0
4.0
3.0
2.0
1.0
0.001
0.01
0.10
1.0
10.0
Λ = ω/Ω,

Figure 1

G65-292

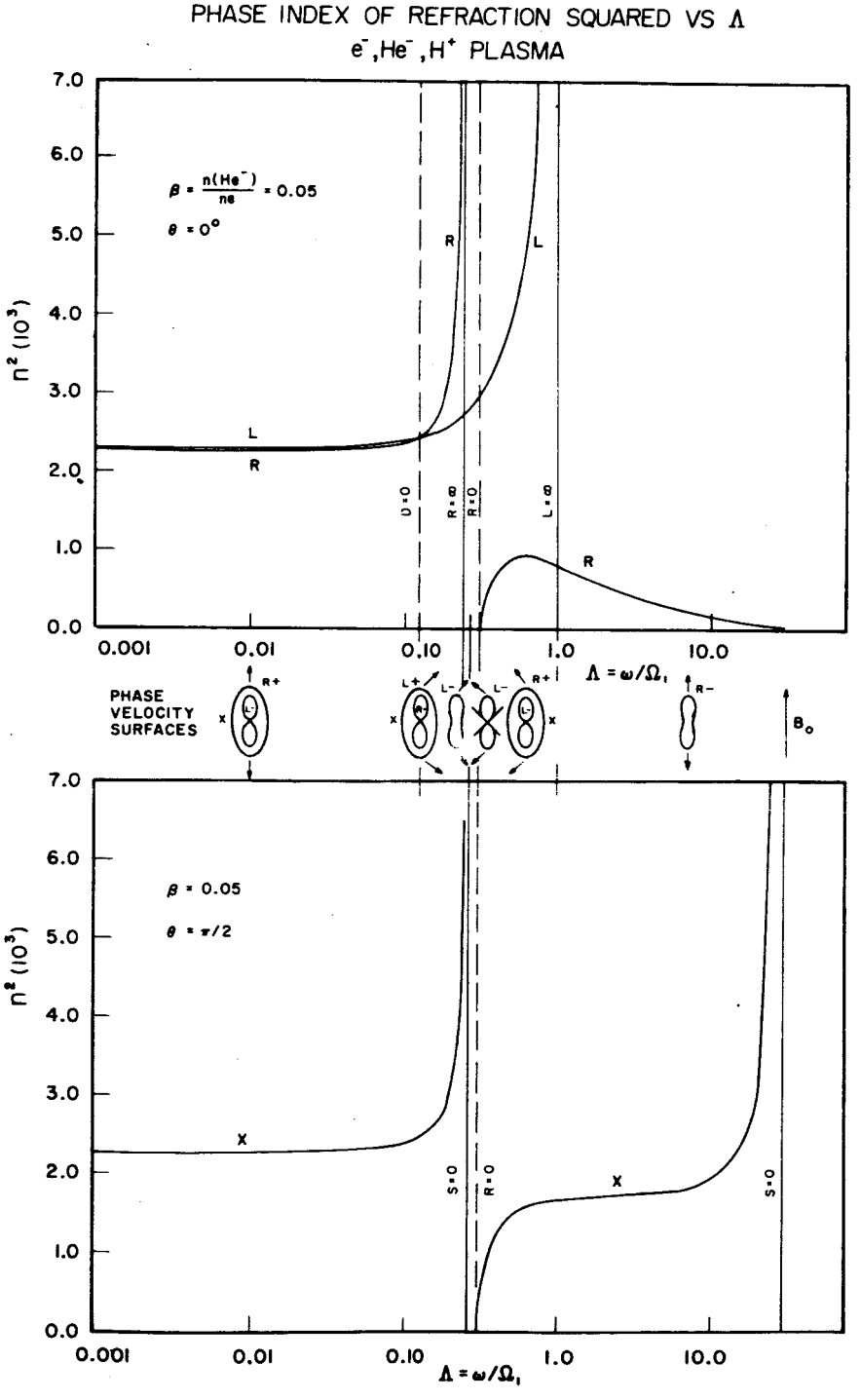

Figure 2

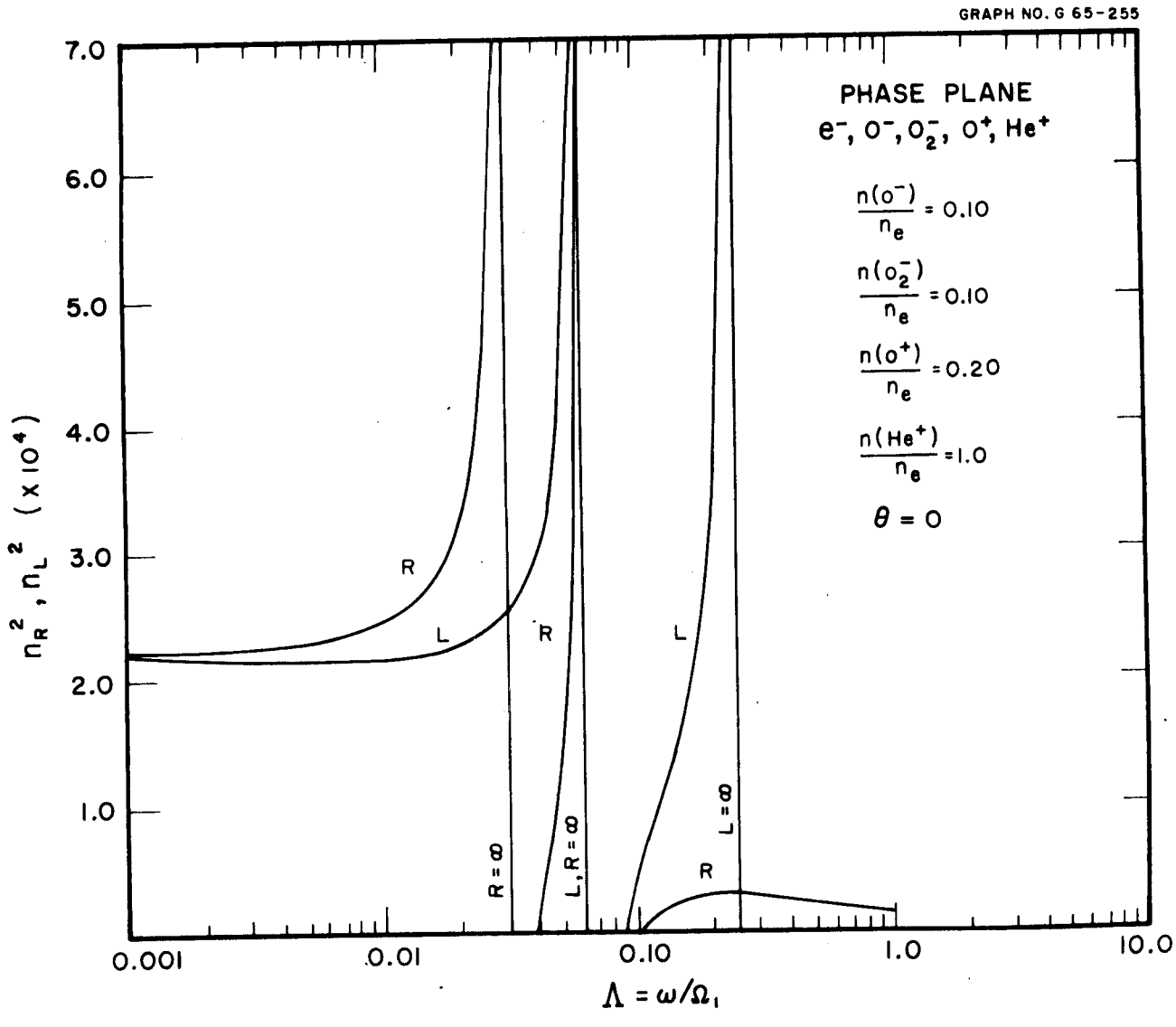
GRAPH NO. G 65-255
PHASE PLANE
e⁻, O⁻, O₂⁻, O⁺, He⁺
n(O⁻)/nₑ = 0.10
n(O₂⁻)/nₑ = 0.10
n(O⁺)/nₑ = 0.20
n(He⁺)/nₑ = 1.0
θ = 0
7.0
6.0
5.0
4.0
3.0
2.0
1.0
n_R², n_L² (X 10⁴)
R
L
R
L
R
R = ∞
L, R = ∞
L = ∞
0.001
0.01
0.10
1.0
10.0
Λ = ω/Ω₁

Figure 3

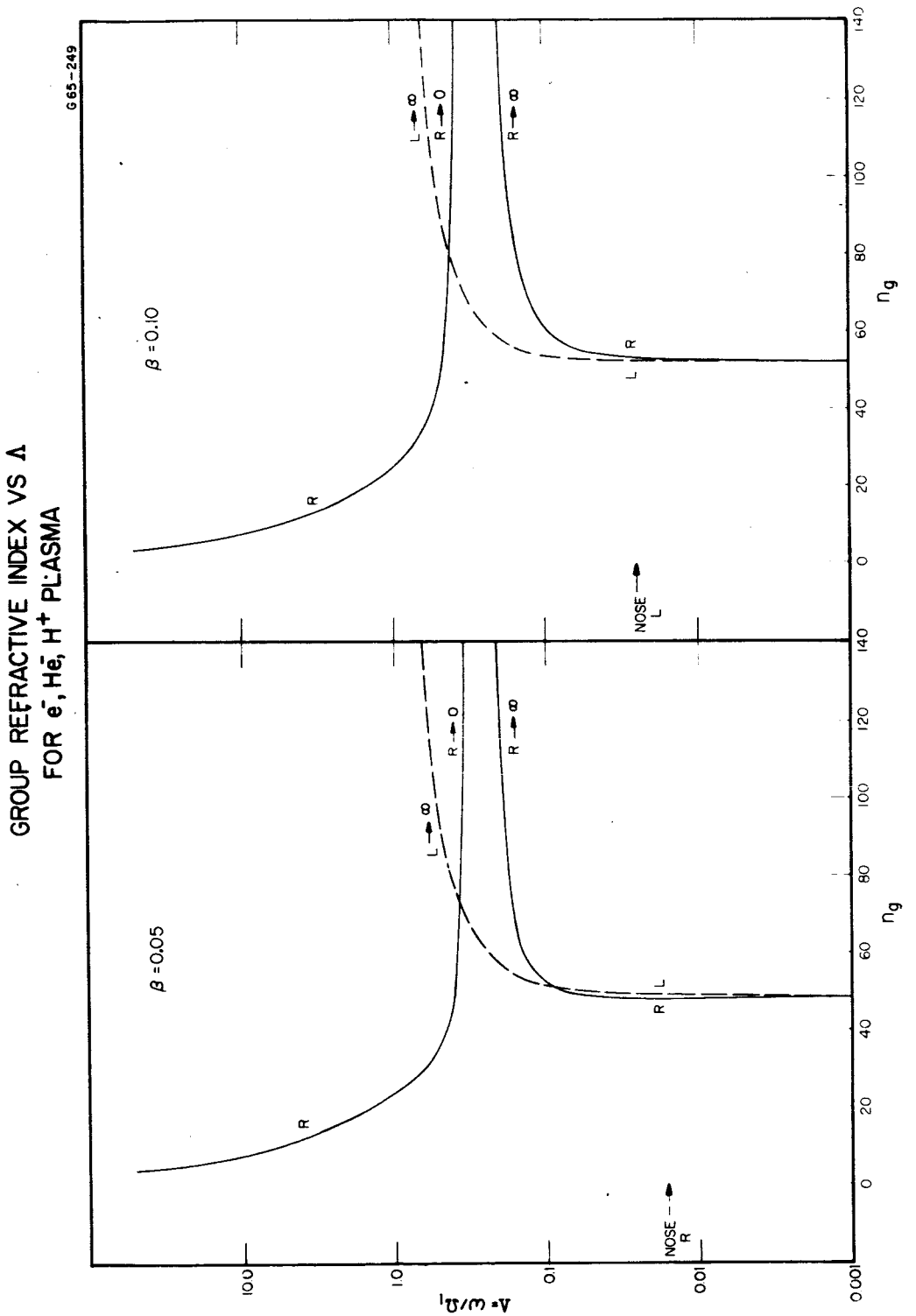
GROUP REFRACTIVE INDEX VS Λ
FOR e⁻, He⁻, H⁺ PLASMA
G65-249
β = 0.10
β = 0.05
R
L
L → ∞
R → 0
R → ∞
NOSE
n_g
Λ = ω/Ω_i
0.001
0.01
0.1
1.0
10.0
0
20
40
60
80
100
120
140

Figure 4

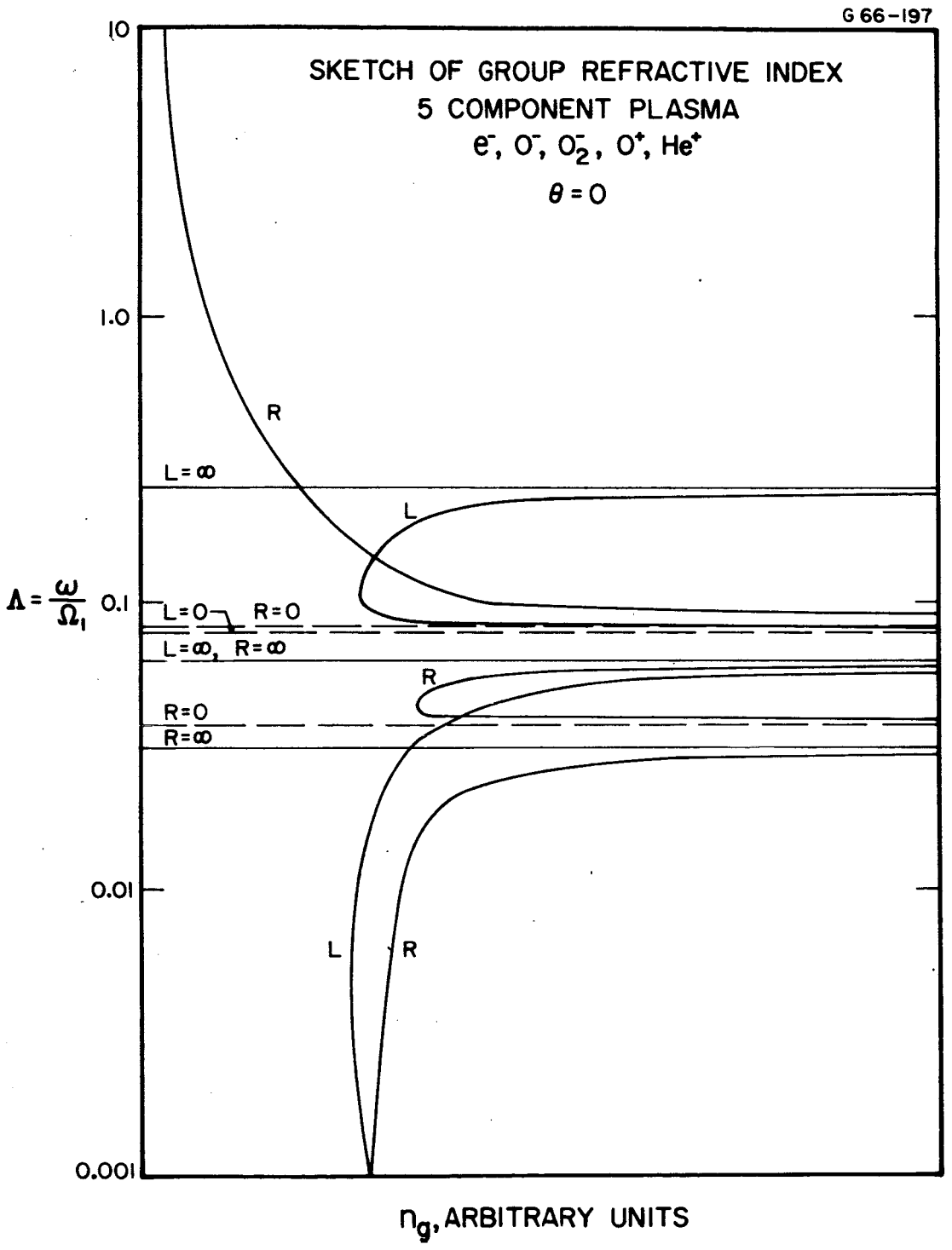
G 66-197
SKETCH OF GROUP REFRACTIVE INDEX
5 COMPONENT PLASMA
e^-, O^-, O_2^-, O^+, He^+
$\theta = 0$
10
1.0
0.1
0.01
0.001
$\Lambda = \frac{\omega}{\Omega_1}$
R
L=∞
L
L=0
R=0
L=∞, R=∞
R
R=0
R=∞
L
R
n_g, ARBITRARY UNITS

Figure 5

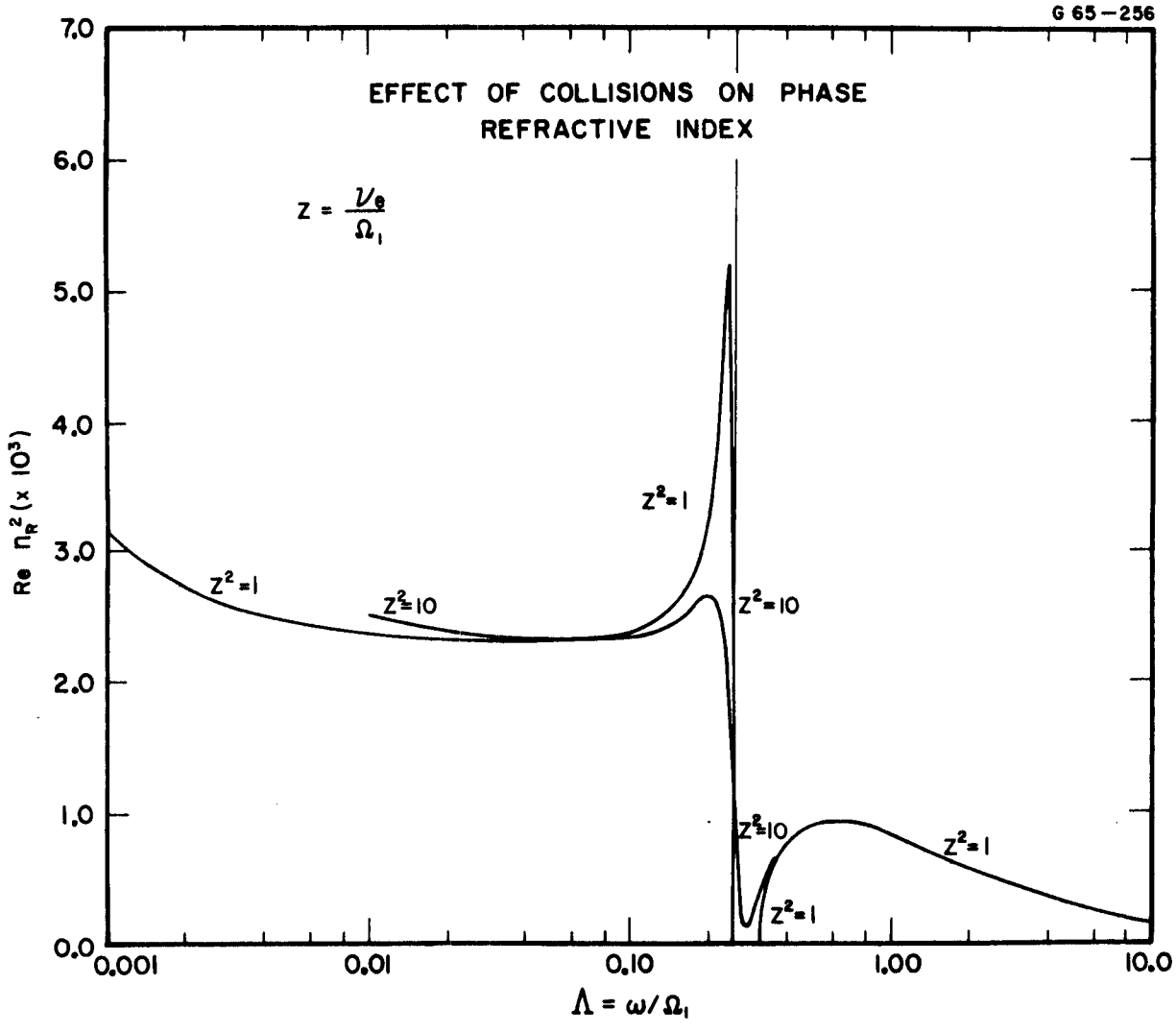
G 65-256
EFFECT OF COLLISIONS ON PHASE REFRACTIVE INDEX
$Z = \frac{\nu_e}{\Omega_1}$
Re n_R^2 (x 10^3)
7.0
6.0
5.0
4.0
3.0
2.0
1.0
0.0
$Z^2=1$
$Z^2=10$
$Z^2=1$
$Z^2=10$
$Z^2=10$
$Z^2=1$
$Z^2=1$
0.001
0.01
0.10
1.00
10.0
$\Lambda = \omega/\Omega_1$

Figure 6

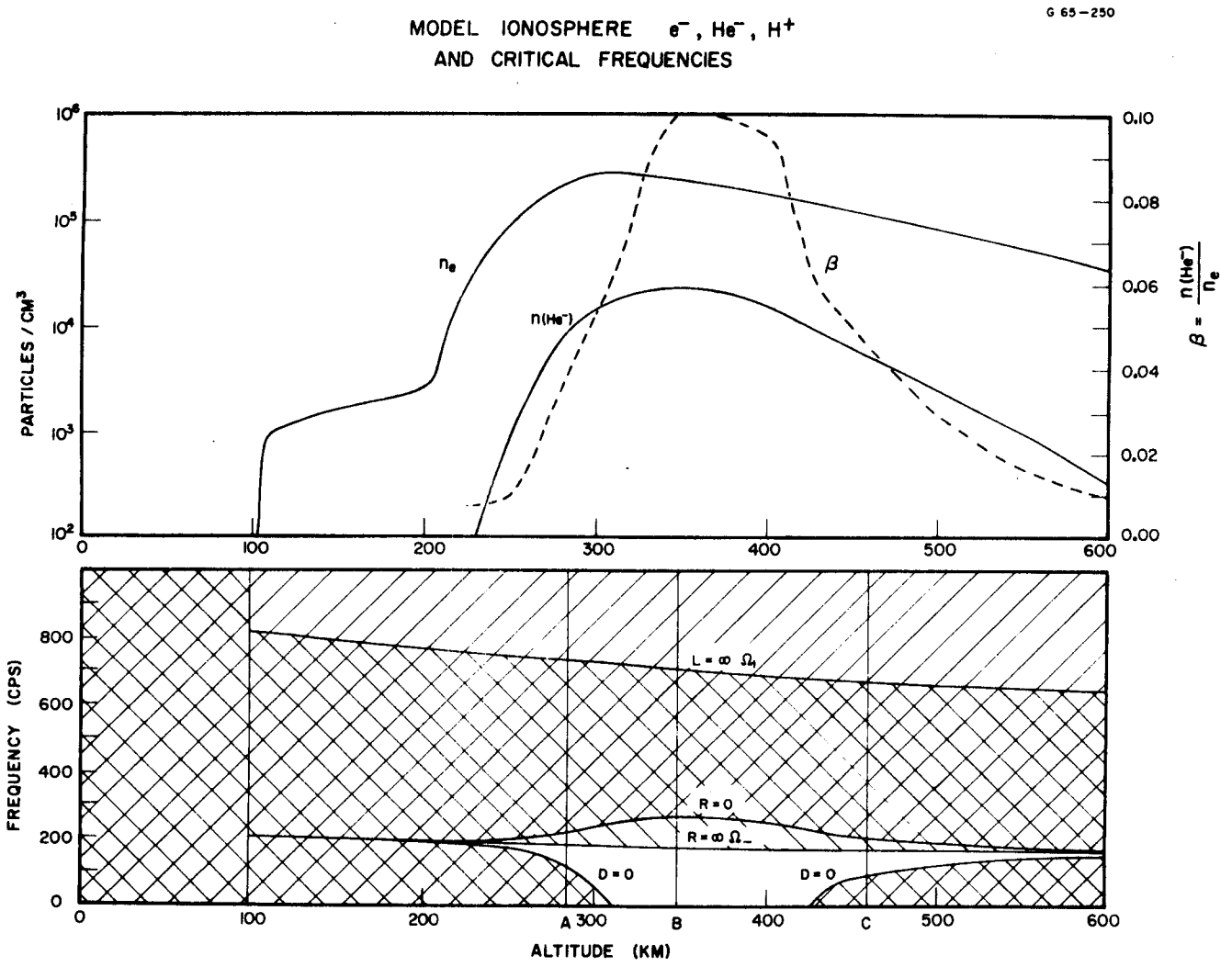
G 65-250
MODEL IONOSPHERE e⁻, He⁻, H⁺
AND CRITICAL FREQUENCIES
PARTICLES / CM³
10^6
10^5
10^4
10^3
10^2
n_e
n(He⁻)
β
$\beta = \frac{n(He^-)}{n_e}$
0.10
0.08
0.06
0.04
0.02
0.00
0
100
200
300
400
500
600
FREQUENCY (CPS)
800
600
400
200
0
L = ∞ Ω_+
R = 0
R = ∞ Ω_-
D = 0
D = 0
A
B
C
ALTITUDE (KM)

Figure 7

G65-248

SPECTROGRAM SKETCHES e^-, He^-, H^+ PLASMA

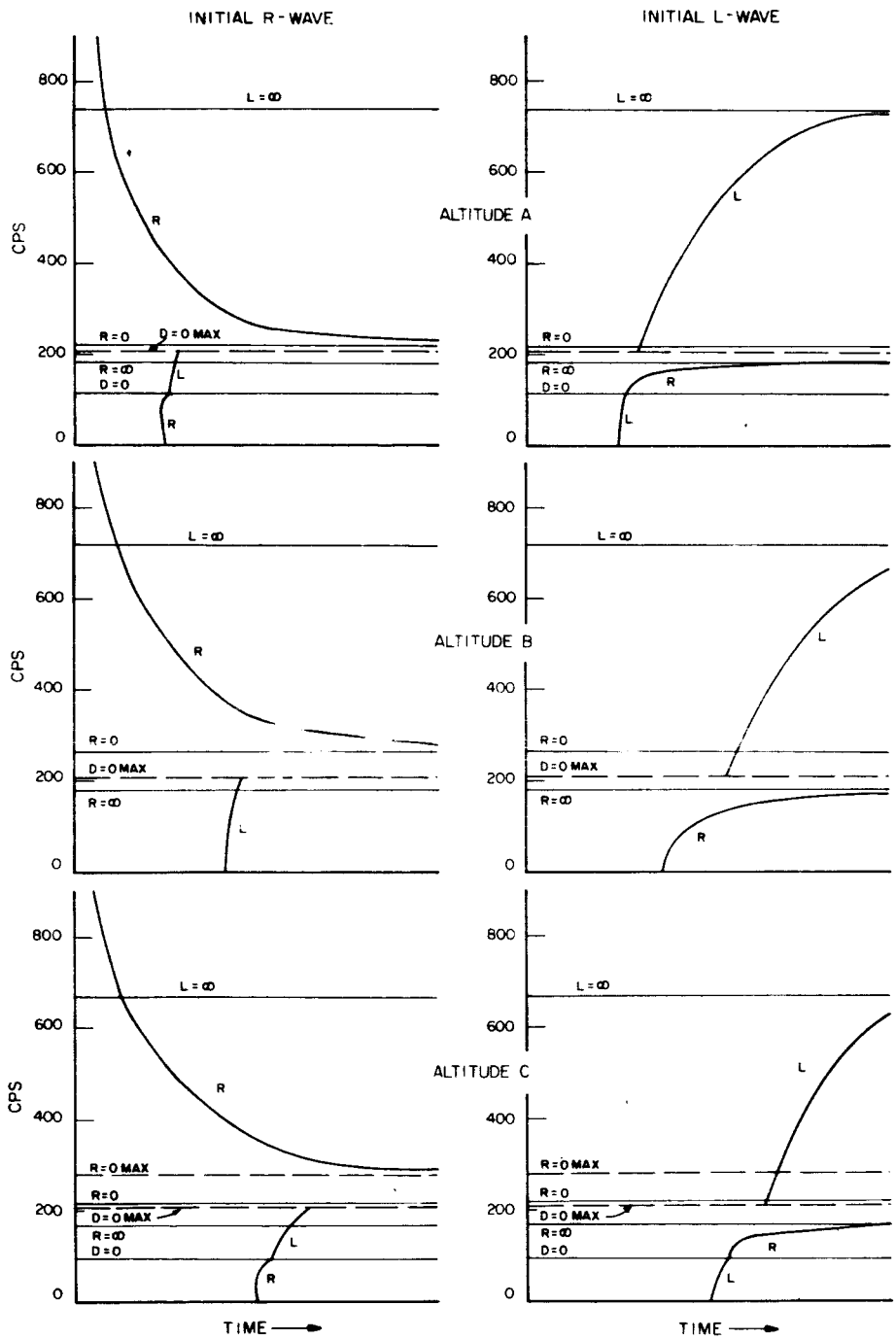

Figure 8

Unclassified

• Security Classification

DOCUMENT CONTROL DATA - R&D

(Security classification of title, body of abstract and indexing annotation must be entered when the overall report is classified)

1. ORIGINATING ACTIVITY (Corporate author)	2a. REPORT SECURITY CLASSIFICATION
University of Iowa	2b. GROUP

3. REPORT TITLE

Negative Ion Detection in the Ionosphere From Effects on ELF Waves

4. DESCRIPTIVE NOTES (Type of report and inclusive dates)

Research Report July 1965 to March 1966

5. AUTHOR(S) (Last name, first name, initial)

Shawhan, Stanley D.

6. REPORT DATE	7a. TOTAL NO. OF PAGES	7b. NO. OF REFS
March, 1966	51	16

8a. CONTRACT OR GRANT NO.	9a. ORIGINATOR'S REPORT NUMBER(S)
N9onr-93803, Nonr 1509(06	University of Iowa 66-11
b. PROJECT NO.	
c.	9b. OTHER REPORT NO(S) (Any other numbers that may be assigned this report)
d.	

10. AVAILABILITY/LIMITATION NOTICES

Unlimited

11. SUPPLEMENTARY NOTES	12. SPONSORING MILITARY ACTIVITY
	Office of Naval Research

13. ABSTRACT

The theory for propagation of small amplitude electromagnetic waves in a cold, homogeneous plasma including negative ions and immersed in a uniform, static magnetic field is developed. It is found that for longitudinal propagation each negative ion introduces a resonance at the negative in gyrofrequency, a concentration dependent cutoff frequency above the negative ion gyrofrequency, and possibly a crossover frequency depending on the ion concentrations and charge to mass ratios. At both the gyrofrequency and the cutoff frequency the group refractive index becomes infinite. Between these two frequencies there is a 'nose' frequency for which the group refractive index is a minimum. Examples are given for a three and five component plasma.

Application of this negative ion theory is made to propagation of negative ion whistlers in the ionosphere. It is found that for frequencies near the negative ion gyrofrequencies the WKB approximation is valid above 300 KM during the nighttime and 150 KM during the daytime. Effects of collisions can be neglected above 150 KM. An ideal experiment is proposed for observation of negative ion whistlers (1-1000 cps). Sample whistler, frequency-time spectrograms like those which would be observed with such an experiment are sketched. From the distinctive frequencies on these sample spectrograms, it is shown that the negative ion specie and concentration can be determined using the developed cold plasma expressions.

DD FORM 1 JAN 64 1473

Unclassified

Security Classification

14. KEY WORDS	LINK A		LINK B		LINK C	
	ROLE	WT	ROLE	WT	ROLE	WT
VLF Propagation Negative Ions Negative Ion Species in Ionosphere Negative Ion Concentration in Ionosphere Phase and Group Refractive Index with Negative Ions						

INSTRUCTIONS

1. ORIGINATING ACTIVITY: Enter the name and address of the contractor, subcontractor, grantee, Department of Defense activity or other organization *(corporate author)* issuing the report.

2a. REPORT SECURITY CLASSIFICATION: Enter the overall security classification of the report. Indicate whether "Restricted Data" is included. Marking is to be in accordance with appropriate security regulations.

2b. GROUP: Automatic downgrading is specified in DoD Directive 5200.10 and Armed Forces Industrial Manual. Enter the group number. Also, when applicable, show that optional markings have been used for Group 3 and Group 4 as authorized.

3. REPORT TITLE: Enter the complete report title in all capital letters. Titles in all cases should be unclassified. If a meaningful title cannot be selected without classification, show title classification in all capitals in parenthesis immediately following the title.

4. DESCRIPTIVE NOTES: If appropriate, enter the type of report, e.g., interim, progress, summary, annual, or final. Give the inclusive dates when a specific reporting period is covered.

5. AUTHOR(S): Enter the name(s) of author(s) as shown on or in the report. Enter last name, first name, middle initial. If military, show rank and branch of service. The name of the principal author is an absolute minimum requirement.

6. REPORT DATE: Enter the date of the report as day, month, year; or month, year. If more than one date appears on the report, use date of publication.

7a. TOTAL NUMBER OF PAGES: The total page count should follow normal pagination procedures, i.e., enter the number of pages containing information.

7b. NUMBER OF REFERENCES: Enter the total number of references cited in the report.

8a. CONTRACT OR GRANT NUMBER: If appropriate, enter the applicable number of the contract or grant under which the report was written.

8b, 8c, & 8d. PROJECT NUMBER: Enter the appropriate military department identification, such as project number, subproject number, system numbers, task number, etc.

9a. ORIGINATOR'S REPORT NUMBER(S): Enter the official report number by which the document will be identified and controlled by the originating activity. This number must be unique to this report.

9b. OTHER REPORT NUMBER(S): If the report has been assigned any other report numbers *(either by the originator or by the sponsor)*, also enter this number(s).

10. AVAILABILITY/LIMITATION NOTICES: Enter any limitations on further dissemination of the report, other than those imposed by security classification, using standard statements such as:

(1) "Qualified requesters may obtain copies of this report from DDC."

(2) "Foreign announcement and dissemination of this report by DDC is not authorized."

(3) "U. S. Government agencies may obtain copies of this report directly from DDC. Other qualified DDC users shall request through _____."

(4) "U. S. military agencies may obtain copies of this report directly from DDC. Other qualified users shall request through _____."

(5) "All distribution of this report is controlled. Qualified DDC users shall request through _____."

If the report has been furnished to the Office of Technical Services, Department of Commerce, for sale to the public, indicate this fact and enter the price, if known.

11. SUPPLEMENTARY NOTES: Use for additional explanatory notes.

12. SPONSORING MILITARY ACTIVITY: Enter the name of the departmental project office or laboratory sponsoring *(paying for)* the research and development. Include address.

13. ABSTRACT: Enter an abstract giving a brief and factual summary of the document indicative of the report, even though it may also appear elsewhere in the body of the technical report. If additional space is required, a continuation sheet shall be attached.

It is highly desirable that the abstract of classified reports be unclassified. Each paragraph of the abstract shall end with an indication of the military security classification of the information in the paragraph, represented as *(TS), (S), (C), or (U)*.

There is no limitation on the length of the abstract. However, the suggested length is from 150 to 225 words.

14. KEY WORDS: Key words are technically meaningful terms or short phrases that characterize a report and may be used as index entries for cataloging the report. Key words must be selected so that no security classification is required. Identifiers, such as equipment model designation, trade name, military project code name, geographic location, may be used as key words but will be followed by an indication of technical context. The assignment of links, roles, and weights is optional.